THE JOURNAL OF PHYSICAL CHEMISTRY B

Article

pubs.acs.org/JPCB

Hydrogen Sulfide Inhibits Amyloid Formation

Manuel F. Rosario-Alomar,[†,⊥] Tatiana Quiñones-Ruiz,[§,⊥] Dmitry Kurouski,[§] Valentin Sereda,[§] Eduardo B. Ferreira,[§] Lorraine De Jesús-Kim,[‡] Samuel Hernández-Rivera,[†] Dmitri V. Zagorevski,[∥] Juan López-Garriga,*[,†] and Igor K. Lednev*[,§]

[†]Department of Chemistry and [‡]Department of Biology, University of Puerto Rico at Mayagüez, Mayagüez, Puerto Rico 00693

[§]Department of Chemistry, University at Albany, SUNY, Albany, New York 12222, United States

[∥]Center for Biotechnology and Interdisciplinary Studies, Rensselaer Polytechnic Institute, Troy, New York 12180, United States

Supporting Information

ABSTRACT: Amyloid fibrils are large aggregates of misfolded proteins, which are often associated with various neurodegenerative diseases such as Alzheimer's, Parkinson's, Huntington's, and vascular dementia. The amount of hydrogen sulfide (H_2S) is known to be significantly reduced in the brain tissue of people diagnosed with Alzheimer's disease relative to that of healthy individuals. These findings prompted us to investigate the effects of H_2S on the formation of amyloids *in vitro* using a model fibrillogenic protein hen egg white lysozyme (HEWL). HEWL forms typical β-sheet rich fibrils during the course of 70 min at low pH and high temperatures. The addition of H_2S completely inhibits the formation of β-sheet and amyloid fibrils, as revealed by deep UV resonance Raman (DUVRR) spectroscopy and ThT fluorescence. Nonresonance Raman spectroscopy shows that disulfide bonds undergo significant rearrangements in the presence of H_2S. Raman bands corresponding to disulfide (RSSR) vibrational modes in the 550−500 cm^{-1} spectral range decrease in intensity and are accompanied by the appearance of a new 490 cm^{-1} band assigned to the trisulfide group (RSSSR) based on the comparison with model compounds. The formation of RSSSR was proven further using a reaction with TCEP reduction agent and LC-MS analysis of the products. Intrinsic tryptophan fluorescence study shows a strong denaturation of HEWL containing trisulfide bonds. The presented evidence indicates that H_2S causes the formation of trisulfide bridges, which destabilizes HEWL structure, preventing protein fibrillation. As a result, small spherical aggregates of unordered protein form, which exhibit no cytotoxicity by contrast with HEWL fibrils.

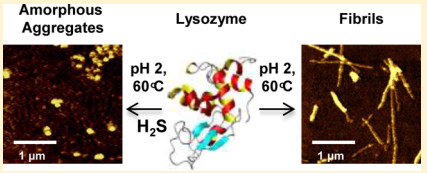

INTRODUCTION

Amyloids are large aggregates of misfolded proteins with a highly stable cross β-structure, which are associated with a variety of degenerative illnesses such as Alzheimer's,[1] Parkinson's,[2] and Huntington's[3] diseases. Proteins with different functionalities and native structures ranging from α-helical and β-sheet rich to intrinsically unordered are able to form amyloid fibrils *in vitro* with a characteristic cross-β core structure.[4−6] This observation leads to the conclusion that protein fibrillation is a generic property of a polypeptide chain. There are numerous research reports demonstrating that a general fibrillation mechanism involves a partially unfolded protein as the first intermediate state.[7,8] Steps to follow include the formation of small aggregates and a β-sheet rich nucleus, which generates further protein aggregation and the formation of mature fibrils.

A reduced amount of hydrogen sulfide (H_2S) in the brain tissue of patients with Alzheimer's disease has been recently reported.[9] For centuries, people have been interested in H_2S for its role as a poisonous chemical. At high concentrations, H_2S inhibits cytochrome *c* and, as a consequence, the electron transport chain.[10] It also binds to hemoglobin forming a sulfhemoglobin complex as detected during sulfhemoglobinemia.[11] More recently, it has been demonstrated that H_2S has gasotransmitter functions, similar to CO and NO.[12] For example, a suspended animation-like state in mice has been achieved by administering ppm levels of H_2S at low temperatures. The metabolic rate and body core temperature decrease and fully recover after such exposure—a promising medical benefit that reduces physiological damage after trauma.[13] In the past two decades, significant attention has been paid to understanding the physiological role of H_2S and its endogenous production. H_2S is biosynthesized in mammalian tissue by nonenzymatic reactions and by the enzymatic degradation of cysteine by cystathione β synthetase (CBS), cystathione γ lyase (CSE), cysteine aminotransferase (CAT), and cysteine lyase (CL).[14] Consumption of garlic induces nonenzymatic H_2S production.[15] Moreover, aged garlic extract has been shown to cause a reduction of *in vivo* Aβ fibrils and soluble amyloid as well as a decrease in tau conformational changes.[16] This indirect evidence concerning the role of H_2S in neurodegenerative diseases has motivated us to investigate the effects of H_2S on the formation of amyloid fibrils.

Small molecules can have a significant effect on the formation of amyloid fibrils. There is extensive literature on the inhibitory activity of various small molecules on protein fibrillation.[17]

Received: August 21, 2014
Revised: December 22, 2014
Published: December 29, 2014

DOI: 10.1021/jp508471v
J. Phys. Chem. B 2015, 119, 1265−1274

Recently, Arioso and coauthors[17] have reviewed the development of amyloid inhibitors, such as antibodies[18] and chaperones,[19] small molecules (e.g., Congo red and polyphenols), colloidal inhibitors, and organic/inorganic nanoparticles, as possible participants in the various states of protein aggregation. These states include the inhibition of primary nucleation (monomer-to-oligomer transition), secondary nucleation (oligomer elongation), and postelongation. However, we have not found any published reports on the role of H_2S in protein aggregation.

It is well documented that H_2S reacts with disulfide bonds, leading one to hypothesize that this reaction could have a significant effect on the mechanism of protein fibrillation. Kumar and co-workers have reported that protecting disulfide bridges with iodoacetamide in an alkaline solution limits the lysozyme fibril growth to 50%.[20] This group has concluded that changing the dynamics of disulfide to *aberrant* disulfide bonds would redirect the process toward the formation of native-like lysozyme aggregates.[20] It has been reported that treating antibodies with H_2S has resulted in SS bond modifications, including the formation of trisulfide bonds (SSS) assessed by liquid chromatography and mass spectrometry (LC-MS).[21] Surprisingly, no changes in antibody stability and function have been observed. H_2S can be incorporated as a sulfane sulfur, a divalent sulfur with six valence electrons, and an oxidation number of zero (S^0) that only binds to other sulfur atoms to form polysulfides.[22] Several research groups have also reported that the sulfur atom of H_2S can be endogenously incorporated into a large amount of proteins by sulfuration, also known as sulfhydration of cysteines. This leads to the formation of protein persulfides (SSH), which could play an intermediary role in protein SSS formation.[23]

In the current study, we have investigated the effect of H_2S on the aggregation of lysozyme, a glycoside hydroxylase responsible for antimicrobial protection in most mammalian species. HEWL is a single chain protein stabilized by four SS bonds in positions Cys6-Cys127, Cys30-Cys115, Cys64-Cys80, and Cys76-Cys94.[24] It was found that H_2S inhibits the formation of HEWL fibrils. The effect of H_2S has been investigated under typical fibrillation conditions such as high temperature and acidic pH using DUVRR and nonresonance Raman spectroscopy, fluorescence, LC-MS, and atomic force microscopy (AFM). We have shown that in the presence of H_2S HEWL forms spherical aggregates of unordered protein under fibrillation conditions. Cytotoxicity tests reveal that these spherical aggregates have no cell toxicity by contrast with typical HEWL fibrils. Our spectroscopic results, buttressed by data that have been published, indicate that H_2S reacts with protein disulfide bonds to form trisulfide bridges. This reaction results in significant lysozyme denaturation and the formation of spherical aggregates of unordered proteins, which prevent protein fibrillation. This discovery indicates possible new roles for H_2S and trisulfide bridges in protein biochemistry *in vivo*.

MATERIALS AND METHODS

The following chemicals were purchased from Sigma-Aldrich (St. Louis, MO): 99.7% acetic acid (695092), sodium chloride (NaCl) (S771-3), HEWL (L6876), sodium sulfidenonahydrate salt (208043), dipropyl disulfide (149225), and trisulfide (6028-61-1).

HEWL Solution Preparation. Lysozyme was dissolved (25 mg/mL) in 20% acetic acid and 100 mM NaCl at pH 2.0 and incubated at 60 °C to form fibrils under initial (control) conditions. To study the effect of H_2S, sodium sulfide nonahydrate salt (12 mM) was added to the control solution in a molar ratio of 1:5 (HEWL:H_2S), prior to the temperature elevation.

Nonresonance Raman Experiments. Powder samples of native and aggregated HEWL were prepared by drying the solutions under nitrogen at room temperature, which removed the acetic acid. Raman spectra (785 nm excitation) of HEWL powder samples and pure dipropyl di- and trisulfide liquids were recorded using a Renishaw inVia confocal Raman spectrometer equipped with a research grade Leica microscope and 50× objective (numerical aperture, 0.55). Five accumulations of 30 s each were collected for each sample in the range of 400−1800 cm^{-1}. Wire 4.0 software was used for data collection. A laser power of approximately 11.5 mW was used to avoid sample photodegradation.

TCEP Test for Trisulfides. A reaction with tris(2-carboxyethyl)phosphine (TCEP) reducing agent was used as a test for trisulfides.[25] Hen egg white lysozyme (HEWL) in native and aggregated form was incubated at pH 2.0 and room temperature for 90 min in the presence of TCEP. The reaction products were analyzed using LC-MS and normal Raman spectroscopy. LC-MS experiments were performed on Thermo LTQ Orbitrap XL mass spectrometer (Thermo, Bremen, Germany). Samples were injected using an Agilent 1200 nano-HPLC system (Agilent, Palo Alto, CA) and Agilent 1200 autosampler. Agilent Zorbax C18 column (150 × 4.6 mm) was used for separation of mixtures. The injection volume was up to 8 μL, and a flow rate of the mobile phase was 250 μL/min. Mobile phase consisted of 0.2% of formic acid (solvent A) and 0.2% formic acid in acetonitrile (solvent B) with the gradient from 5% to 40% of solvent B in 40 min followed by washing the column by 90% of solvent B and equilibration. The mass spectrometer operated in ESI mode in the mass range m/z 100−500 with detection of positively and negatively charged ions. The resolution was ∼30 000, and the accuracy of mass measurements was better than 2 ppm.

Powder samples of HEWL aggregates incubated at different concentrations of TCEP were prepared for nonresonance Raman spectroscopic analysis by drying the corresponding solutions under a nitrogen flow at room temperature.

Deep UV Resonance Raman Spectroscopy (DUVRR). DUVRR spectra (199.7 nm excitation) of 25 mg/mL HEWL were collected using a home-built instrument equipped with a CCD camera (Roper Scientific, Inc.) cooled in liquid nitrogen.[26] A spinning quartz NMR tube with a magnetic stirrer was used for sampling. Each spectrum recorded an average of 20 accumulations with 30 s acquisition time. GRAMS/AI 7.0 software (Thermo Galactic, Salem, NH) was used for data processing.

Tryptophan and ThT Fluorescence. Fluorescence spectra were measured in a JobinYvon Fluoromax-3 spectrofluorometer (JobinYvon, Edison, NJ). Intrinsic tryptophan fluorescence of 25 mg/mL HEWL was measured in a 10 μm path length cell without dilutions. The UV absorption was <0.05 at an excitation wavelength of 295.5 nm. The excitation and emission slits were 0.5 and 5 nm, respectively. Three spectral accumulations were taken, and the spectra were averaged for each sample. HEWL fibrils formed after 90 min of incubation were also characterized using intrinsic tryptophan fluorescence. Fibrils were washed in acetic acid solution twice in a procedure which included sonication for 10 min, centrifugation for 4 min

DOI: 10.1021/jp508471v
J. Phys. Chem. B 2015, 119, 1265−1274

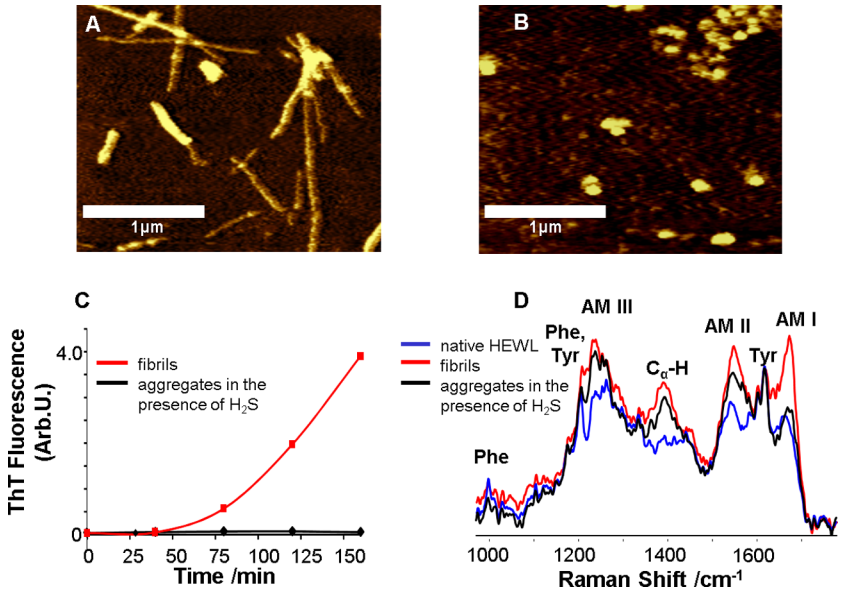

Figure 1. Lysozyme forms β-sheet-rich fibrils under fibrillogenic control conditions and spherical aggregates of unordered protein under fibrillogenic conditions with H_2S incubation. AFM images of (A) HEWL fibrils formed after incubation of the control solution for 90 min and (B) HEWL aggregates formed after incubation of the solution in the presence of H_2S for 48 h; scale bars are 1 μm. (C) Aggregation kinetics (ThT fluorescence) of HEWL incubated under control conditions (red) and in the presence of H_2S (black). (D) DUVRR spectra of native HEWL (blue), HEWL fibrils (red) and HEWL spherical aggregates (black) formed in the presence of H_2S; all spectra were normalized using the aromatic amino acid Raman band (approximately 1600 cm^{-1}) for comparison. The amide I vibrational mode (Am I) is dominated by C═O stretching, with minor contributions from C−N stretching and N−H bending.[28] Amide II (Am II) and amide III (Am III) bands involve significant C−N stretching, N−H bending, and C−C stretching.[29] The Cα−H bending vibrational mode involves Cα−H symmetric bending and C−Cα stretching.[30]

at 13 000 rpm, the removal of supernatant liquid, and resuspension in an acetic acid solution.

In the ThT fluorescence assay, aliquots of 25 mg/mL HEWL were diluted in a molar ratio of 1:10 (HEWL:Thioflavin T (ThT) dye) to a final concentration of 2.5 mM ThT. The excitation and emission wavelengths were 450 and 480 nm, respectively. The excitation and emission slits were 5 nm. Three recorded spectra were averaged for each measurement.

Atomic Force Microscope. Aliquots of HEWL incubated at 60 °C, pH 2.0, 100 mM NaCl, were cooled to room temperature and deposited on freshly cleaved mica. After a few minutes of exposure, the mica surface was rinsed with MQ water and dried. AFM images were collected using the SmartSPM 1000 system (AIST-NT, Novato, CA). Images were acquired in the tapping mode using silicon cantilevers with a 10−25 nm tip curvature radius.

Cell Culture. Human neuroblastoma SH-SY5Y cells were cultured in a 1:1 (v/v) mixture of DMEM (Sigma-Aldrich, St. Louis, MO) and Ham's F-12 nutrient mixture (Sigma-Aldrich, St. Louis, MO) supplemented with 10% FBS (Sigma-Aldrich, St. Louis, MO) and Antibiotic-Antimitotic Solution (Sigma-Aldrich, St. Louis, MO). The cells were incubated at 37 °C in an incubator with 95% humidified air and 5% CO_2.

MTT Reduction Assay. Cells were plated onto flat-bottom 96-well plates (1×10^4 cells per well) and incubated overnight at 37 °C. After cell attachment, the initial medium was replaced with serum-free medium using different concentrations of mature HEWL fibrils or HEWL aggregates (formed with H_2S) and incubated for 24 h. Cytotoxicity was assessed using the MTT reduction inhibition assay.[27] MTT was added to the culture medium to yield a final concentration of 0.5 mg/mL. Cells were incubated with the MTT medium for 4 h in a CO_2 incubator, followed by the addition of 200 μL of an isopropanol 0.04 N HCl solution to dissolve formazan crystals. Absorbance was measured at 540 nm using a Synergy H1 plate reader (BioTek, Vermont). Control experiments were performed by exposing cells to solutions of an equivalent volume of the same initial buffer for the same length of time. Cell viability was measured relative to control cells that were not exposed to the HEWL aggregates/HEWL fibrils solutions.

RESULTS

Aggregation and Structural Rearrangements of Lysozyme. To form fibrils, HEWL was incubated at 60 °C in 20% acetic acid (pH 2.0) and 100 mM NaCl, from here on referred to as control conditions. The morphology of lysozyme aggregates formed in the course of incubation under the fibrillogenic conditions and in the presence of H_2S was characterized by AFM. The presence of typical long rodlike fibrils was evident after 90 min of incubation under control conditions (Figure 1A). However, incubation of HEWL in the presence of H_2S resulted in the formation of spherical aggregates instead of fibrils, as evident from AFM images (Figure 1B).

ThT fluorescence is used often to monitor the formation of amyloid fibrils. ThT fluorescence intensity increased dramatically after 70 min of incubation of lysozyme under control conditions, indicating the formation of amyloid fibrils (Figure 1C). However, no increase in ThT fluorescence intensity was observed for the HEWL solution incubated with H_2S within 48 h.

We investigated changes in the lysozyme secondary structure during incubation with and without H_2S using deep UV resonance Raman (DUVRR) spectroscopy. DUVRR has been used to study structural rearrangements of HEWL at all stages of fibrillation.[26,31,32] The DUVRR spectrum of HEWL excited at 199.7 nm was mainly composed of the amide chromosphere and the aromatic amino acid (Phe and Tyr) contributions.[33] A

DOI: 10.1021/jp508471v
J. Phys. Chem. B 2015, 119, 1265−1274

noticeable increase in the intensity and sharpness of the Am I band (approximately 1672 cm^{-1}) indicated the appearance of β-sheets due to the formation of fibrils.[26,34−36] The DUVRR spectrum of fibrillated lysozyme under control conditions confirmed the formation of β-sheets. The spectrum of HEWL after 30 min of incubation under control conditions (Figure 1D, red) is similar to that reported previously for HEWL fibrils.[26]

However, the DUVRR spectrum of lysozyme incubated in the presence of H_2S confirmed the lack of β-sheet formation. In this case, the Am I band (approximately 1670 cm^{-1}) did not show a significant intensity change (Figure 1D, black). Instead, the Am I band shifted slightly to a higher frequency, signifying the formation of an unordered protein.[26,28] This was further supported by the increase in C_α−H band intensity at 1390 cm^{-1} that was indicative of α-helix melting.[37] A significant change in Raman bands for Am III (approximately 1250 cm^{-1}) and Am II (approximately 1555 cm^{-1}) was consistent with the transition of α-helix to unordered protein. Therefore, AFM, ThT fluorescence and DUVRR spectroscopy indicated the formation of unordered spherical aggregates of HEWL by contrast with β-sheet-rich fibrils in the presence of H_2S.

Intrinsic Tryptophan Fluorescence Marker of the Tertiary Structural Rearrangement. Tryptophan (Trp) fluorescence is an efficient intrinsic marker of local environments, which is often used for monitoring tertiary structural changes in proteins.[33] Native lysozyme at neutral pH shows a maximum Trp emission at 340 nm.[38] At pH 2.0 (20% acetic acid), the Trp fluorescence peak shifts to 345 nm, indicating a partial denaturation of lysozyme. A further minor shift to 347 nm due to HEWL fibril formation under control conditions was observed (Figure 2B,C). To confirm that the intrinsic Trp fluorescence is dominated by the signal from HEWL fibrils, the solutions (after incubation for 40 and 90 min) were sonicated, centrifuged and resuspended in 20% acetic acid to remove possible monomeric and oligomeric forms of the protein (Figure 2B).

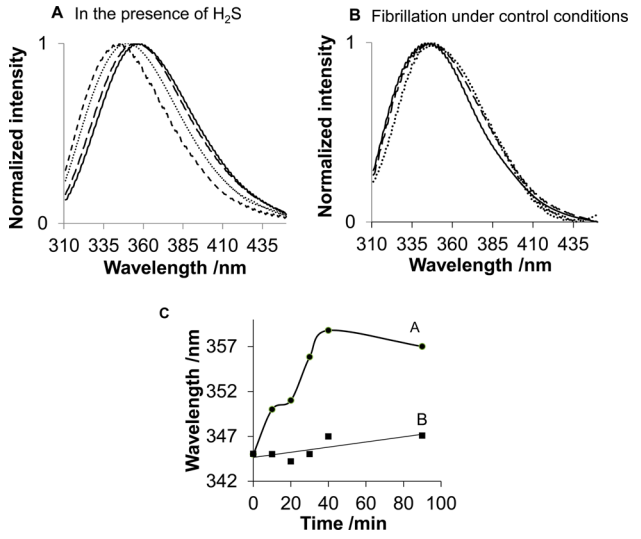

Figure 2. Time-dependent Trp fluorescence changes of lysozyme (A) incubated in the presence of H_2S for 0 min (- - -), 10 min (···), 90 min (– –), and 48 h (—) and (B) incubated with control solution for 0 min (—), 40 min – –), and 90 min (···). (C) Trp maximum emission wavelength of HEWL incubated with H_2S (A, ●) and fibrillation under control conditions (B, ■).

A significant shift of the Trp emission maximum, from 345 to 357 nm, was observed after 90 min of lysozyme incubation in the presence of H_2S (Figure 2A,C), with no further changes for at least 48 h. This significant red-shift is consistent with the previously reported maximum emission at 352 nm for fully denatured lysozyme in 6 M guanidinium-HCl at pH 7.0.[39] Therefore, we conclude that incubation of lysozyme in the presence of H_2S results in a stronger denaturation than that which occurs during control fibrillation conditions.

Rearrangement of Disulfide Bonds. Nonresonance Raman spectroscopy of proteins offers a unique opportunity for characterizing the conformation of disulfide bridges.[35] The SS symmetric stretching[35,40] vibrational mode is typically represented as a strong Raman band in the range of 505−550 cm^{-1}. The Raman spectrum of HEWL was found to change significantly in the SS signature region with incubation time (Figure 3A). A strong 507 cm^{-1} peak in the Raman spectrum of

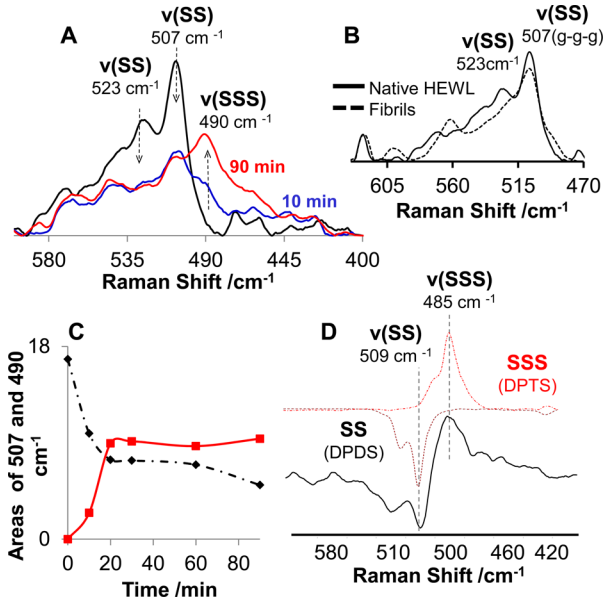

Figure 3. Evolution of lysozyme disulfide bonds in the presence of H_2S probed by normal Raman spectroscopy. Raman spectra of HEWL incubated (A) in the presence of H_2S and (B) under control conditions, where 507 and 523 cm^{-1} bands correspond to g-g-g and g-g-t SS configurations, respectively. Synchronous kinetic change in the area of the 507 and 490 cm^{-1} bands is assigned to the newly formed RSSSR group. (C) Kinetics of RSSSR formation (490 cm^{-1}) and the decrease in the amount of RSSR (507 cm^{-1}) during the incubation of HEWL in the presence of H_2S. (D) Difference spectrum between normal Raman spectra of HEWL aggregated in the presence of H_2S acquired at 90 and 0 min incubation (shown in (A), gray solid line). The latter spectrum is represented by the expected spectral change demonstrating the disulfide-to-trisulfide transition symbolized by the inverted Raman spectrum of dipropyl disulfide (- · -) and dipropyl-trisulfide (red ···).

native HEWL represents the gauche−gauche−gauche (g-g-g) configuration of three SS bonds, and a small 523 cm^{-1} peak can be attributed to the gauche−gauche−trans (g-g-t) configuration of the fourth SS bond of lysozyme.[35,41] The amplitudes of these peaks decreased, and a new peak appeared at 490 cm^{-1} as a result of HEWL incubation in the presence of 12 mM H_2S, indicating significant rearrangements of SS bonds (Figure 3A).

The concentration of 12 mM H_2S corresponded to a 5:1 (H_2S:HEWL) molar ratio, chosen so that a sufficient number of

DOI: 10.1021/jp508471v
J. Phys. Chem. B 2015, 119, 1265−1274

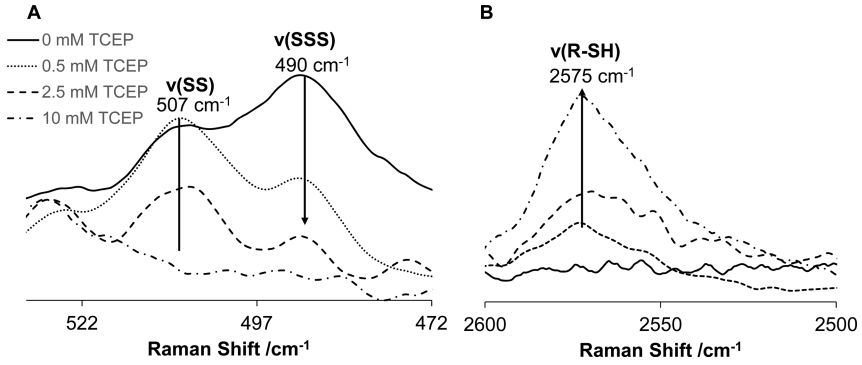

Figure 4. Normal Raman spectra of HEWL aggregates in the presence of reducing agent TCEP with concentration 0 mM (—), 0.5 mM (···), 1 mM (- - -), 2.5 mM (– –), and 10 mM (- · -). Selected spectral regions with characteristic Raman bands of disulfide and trisulfide moieties (A) as well as sulfhydryl (−SH) group (B) are shown. The phenylalanine Raman band at 1003 cm^{-1} was used to normalize the spectra (spectral region not shown).

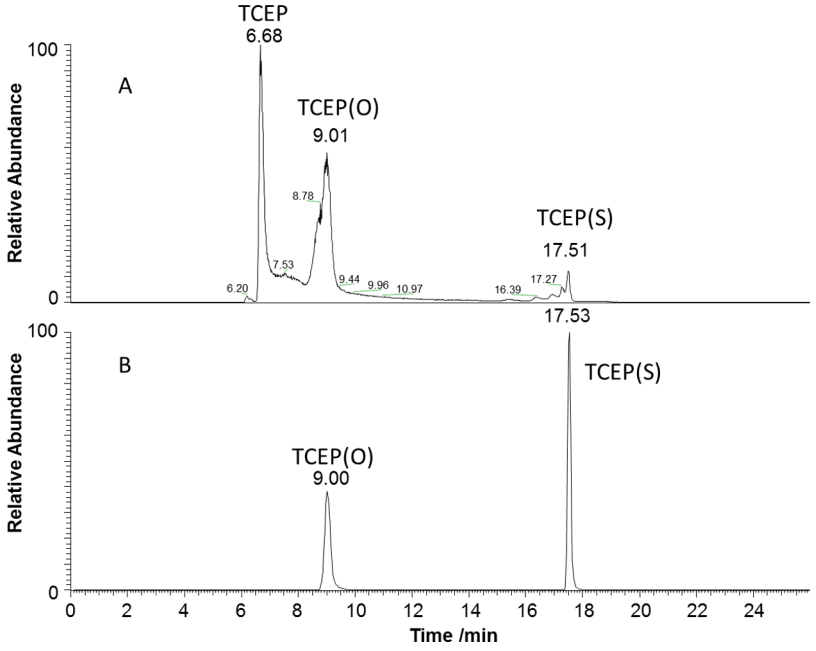

Figure 5. Combined LC-MS (ESI in negative ion mode) chromatograms of ions at m/z 249, m/z 265, and m/z 281 corresponding to deprotonated TCEP, TCEP(O), and TCEP(S), respectively, for native lysozyme incubated with 10 mM TCEP (A) and lysozyme aggregates incubated with 0.5 mM TCEP (B).

H_2S molecules could react with all four lysozyme SS bonds assuming a 1:1 stoichiometric ratio. We are currently investigating the effect of H_2S concentrations. The 1003 cm^{-1} peak corresponding to phenylalanine[42] was used to normalize Raman spectra in Figure 3A (region not shown). Figure 3C shows synchronous kinetic change in the area of the 507 and 490 cm^{-1} bands with incubation time up to 90 min. No further changes were observed during 48 h of additional incubation in the presence of H_2S (data not shown). As discussed in detail below, the dipropyl trisulfide (DPTS) Raman spectrum contains a 485 cm^{-1} band (Figure 3D) characteristic of the trisulfide moiety that motivated us to investigate the possibility of assigning the 490 cm^{-1} band in the HEWL aggregate Raman spectrum to the SSS group. The nonresonance Raman spectroscopy of HEWL fibrillation under control conditions indicates that the 507 cm^{-1} peak does not change significantly during fibril formation (Figure 3B). Therefore, in the absence of H_2S, the HEWL SS bands remain intact and the g-g-g conformation dominates, in agreement with our previous report.[43]

Reduction of Trisulfide Bridges by TCEP. To test the hypothesis about the formation of trisulfide groups, we investigated the reaction of HEWL aggregates with TCEP reduction agent by normal Raman spectroscopy and mass spectrometry. TCEP reaction with SS groups is well-known to result in oxidation of TCEP and formation of TCEP(O) and R−SH groups.[44] More recently, Cumnock et al. reported that TCEP reacted preferentially with SSS moieties in the presence of SS bridges until the majority of SSS groups were consumed according to eqs 1 and 2.[25] SS bridges and thiophosphine TCEP(S) species are main products of the TCEP−SSS reaction.[25] Figure 4 shows Raman spectra of HEWL aggregates after incubation with different concentrations of TCEP (0.5, 1, 2.5, and 10 mM). The amount of aggregated HEWL molecules in these samples was kept about 3.0 mM.

$$\text{TCEP} + \text{R−SSS−R} \rightarrow \text{TCEP(S)} + \text{R−SS−R} \quad (1)$$

DOI: 10.1021/jp508471v
J. Phys. Chem. B 2015, 119, 1265−1274

$$\text{TCEP} + \text{R}{-}\text{SS}{-}\text{R} \rightarrow \text{TCEP(O)} + 2\text{R}{-}\text{SH} \quad (2)$$

The Raman spectrum of HEWL aggregates was found to change significantly in the SSS/SS vibrational signature region with the addition of TCEP (Figure 4A). The SSS band at 490 cm^{-1} decreases after 0.5 mM TCEP addition which is in a good agreement with predominant reaction of TCEP with SSS groups. The amplitudes of both 490 and 507 cm^{-1} bands (SSS and SS, respectively) decreased as a result of HEWL incubation in the presence of higher concentration of TCEP (1−10 mM), indicating significant reduction of SS and SSS groups and formation of R−SH moiety in agreement with an increase in 2575 cm^{-1} band intensity (Figure 4B).

LC-MS was utilized to monitor the formation of TCEP(S) and TCEP(O) as products of SSS and SS reduction, respectively (eqs 1 and 2). The reduction of native HEWL with an excess of TCEP (10 mM) resulted in products with retention times of 6.68, 9.01, and traces at 17.51 min (Figure 5A). Accurate mass measurements confirmed that the products correspond to TCEP, TCEP(O), and TCEP(S), respectively. HEWL aggregates treated with 0.5 mM TCEP showed TCEP(O) and TCEP(S), with retention times of 9.0 and 17.53 min (Figure 5B). All initial TCEP was completely consumed due to the reaction with SSS and SS groups.

The solution of native HEWL incubated with an excess of TCEP contained significant amounts of TCEP and TCEP(O) and traces of TCEP(S). The main expected products of TCEP reaction with RSSR are TCEP(O) and 2RSH.[44] We believe that the traces of TCEP(S) could form due to a prolonged exposure of native HEWL to the excess of TCEP prior to LC-MS analysis. This suggestion is based on the reported reaction 3 of triphenylphosphine (Ph_3P) with dialkyl disulfides (RSSR), which resulted in formation of $Ph_3P(S)$.[45] We hypothesize that the trace amount of TCEP(S) is formed in the reaction of TCEP with native HEWL due to a similar mechanism. However, the amount of TCEP(S) is low because the second step in reaction 3 is slow and reaction 2 dominates.

$$\text{RSSR} + \text{Ph}_3\text{P} \overset{\text{fast}}{\longleftrightarrow} \text{Ph}_3\text{P}^+{-}\text{SR} + \text{RS}^- \overset{\text{slow}}{\longrightarrow} \text{RSR} + \text{Ph}_3\text{P(S)} \quad (3)$$

Overall, the analysis of reaction products resulting from the incubation of native and aggregated lysozyme in the presence of TCEP using LC-MS is consistent with the presence of SSS in aggregated HEWL. The variation in the amplitude of the 490 cm^{-1} Raman band with the concentration of TCEP is in agreement with its assignment to the SSS group as well.

Cytotoxicity of HEWL Incubated with H_2S. To compare the cytotoxicity of HEWL fibrils and spherical aggregates formed in the presence of H_2S, the MTT reduction assay in SH-SY5Y neuroblastoma cells was used. Samples of mature fibrils and spherical aggregates were posteriorly transferred to PBS buffer at pH 7.4 in order to avoid drastic changes in the pH of the cells. To achieve this, mature fibrils were washed three times in PBS buffer, and spherical aggregates were dialyzed against PBS buffer. The latter procedure did not change fibrils and spherical aggregates according to their normal Raman spectra (data not shown). Specifically, the 490 cm^{-1} band remained intact after buffer exchange to PBS. The incubation of confluent SH-SY5Y cells with mature fibrils (0.5−36 μM) for 24 h resulted in a significant reduction (40%) of the cellular viability. By contrast, spherical aggregates showed no detectable cytotoxicity (Figure 6).

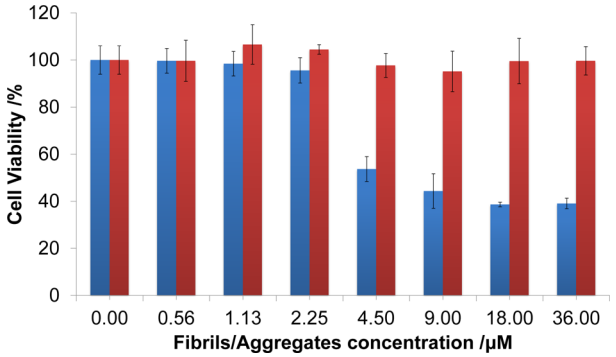

Figure 6. Cytotoxicity of HEWL fibrils (blue) and spherical aggregates (red). Mean cell viability and one standard deviation of two independent experiments performed in triplicate are presented.

DISCUSSION

Evaluation of Lysozyme Secondary and Tertiary Structure. Lysozyme fibril formation has been extensively studied and characterized.[26,31,46] The most common methods used for studying the fibrillation process include AFM, ThT, and Trp fluorescence. DUVRR spectroscopy has been shown to be uniquely suitable for the structural characterization of proteins at all stages of the fibrillation process.[37] We utilized these complementary methods for studying the effect of H_2S on the morphology and structure of lysozyme aggregates. Although fibril formation was not detected by AFM and ThT fluorescence assays, the intrinsic Trp fluorescence marker suggested that significant tertiary structure changes had taken place minutes after H_2S incubation began. The red-shift of Trp fluorescence of greater than 10 nm is typical for unfolded lysozyme.[26] Changes were also evident for SS bridges at the same time scale, as discussed in the next section. The changes observed in the tryptophan local environment and in SS bonds indicate substantial changes in HEWL tertiary structure.

DUVRR spectroscopy was utilized to investigate changes in HEWL secondary structure during the incubation with and without H_2S. It was found that H_2S prevented the formation of β-sheet and resulted in a significant transition of α-helix to unordered protein. Moreover, we utilized DUVRR spectra of aggregated lysozyme to evaluate the protein secondary structure composition. Xu et al.[26] have reported on the quantitative analysis of lysozyme DUVRR spectral changes during its denaturation. According to that work, the amount of α-helix melting can be estimated from the intensity of C_α−H bending band. This band is conveniently isolated from other Raman bands. β-Sheet and unordered structures only contribute to C_α−H bending DUVRR band, while the α-helix does not make a noticeable input.[37] It is evident from amide I Raman bands in DUVRR spectra presented in Figure 1D that no fibril-type β-sheet is formed in HEWL aggregates since the Am I intensity does not increase. Therefore, the increase in the C_α−H band intensity in the spectrum of HEWL aggregates relative to that of native protein could be assigned to newly formed unordered structures. We normalized the DUVRR spectra of HEWL aggregates and native protein with the denatured-reduced HEWL spectrum reported by Xu et al.[26] and estimated the amount of α-helix in HEWL aggregates as 11%. Assuming that the amount of β-sheet in HEWL aggregates is approximately the same as in the native protein, we estimated the secondary structural composition of HEWL aggregates as 83% unordered, 11% α-helix, and 6% β-sheet.

DOI: 10.1021/jp508471v
J. Phys. Chem. B 2015, 119, 1265−1274

To summarize the results concerning the significant tertiary structural rearrangements, α-helix melting, and lack of β-sheet formation, we conclude that H_2S causes more significant denaturation of lysozyme than that taking place during the initial stages of protein fibrillation, which is typically reported as *partial* protein denaturation.[26] We hypothesize that this significant lysozyme denaturation results in rapid protein aggregation, the formation of spherical species, and the prevention of the formation of β-sheets and fibrillation. In other words, H_2S redirects the process to "off-pathway" aggregation, preventing fibril formation.[8,47,48] This observation is consistent with an earlier report by Wang and colleagues which demonstrated that fully denatured lysozyme forms amorphous aggregates that prevent fibril formation.[49] The protein has been fully denatured by reducing SS bonds with DTT_{red}. As a result, fully denatured lysozyme may lack the hydrophobic regions which are present in the partially unordered intermediates formed at the early stage of fibril formation. In addition, it is possible that amorphous aggregates decreased the effective concentration of HEWL available for fibril formation.[49] In agreement with Wang's report, our results suggest that lysozyme denatures strongly in the presence of H_2S and forms unordered aggregates that prevent β-sheet formation and fibrillation.

Formation of Trisulfide Bridges. According to Figure 3, the contributions of both g-g-g (507 cm^{-1} band) and g-g-t (523 cm^{-1} band) conformations of SS bonds to the Raman spectrum of HEWL decreased significantly during its incubation with H_2S. Simultaneously, a new peak appeared at 490 cm^{-1} (Figure 3A,C). Nielsen and colleagues proposed that SSS bridges can form in proteins in the presence of H_2S via the thiol−disulfide exchange reaction, which is known to occur within cells.[23] We investigated the possibility of assigning a new Raman band at 490 cm^{-1} to the SSS moiety. Initially, we reproduced Raman spectra of two model compounds, dipropyl disulfide (DPDS) and dipropyl trisulfide (DPTS), shown in Figure 3D. In agreement with other published studies,[50,51] these compounds exhibit strong Raman bands at 509 and 485 cm^{-1}, respectively, in agreement with the Raman spectra of native HEWL and HEWL spherical aggregates formed in the presence of H_2S. Furthermore, we obtained the difference spectrum by subtracting HEWL spectra after 0 and 90 min of incubation in the presence of H_2S and compared it to the expected spectral change representing the SS to SSS transition. The latter spectral change is depicted as a combination of dipropyl disulfide and dipropyl trisulfide spectra (Figure 3D). This spectral comparison provides further support for the hypothetical assignment of the 490 cm^{-1} Raman band to the SSS moiety.

Several studies have identified a 490 cm^{-1} Raman band in inorganic compounds and small organic molecules containing SSS,[51−54] and we report the appearance of this band in proteins for the first time. Wieser and Krueger have assigned the 488 cm^{-1} Raman peak of H−SSS−H to a symmetric SS stretch with a contribution from the SSS bend.[54] Freeman has reported the Raman spectra of organic SS and SSS compounds, found in natural products where a strong 485 cm^{-1} stretching band has been observed in cyclic and acyclic trisulfides.[51] Janz et al. have reported Raman spectra of inorganic SSS from BaS_3 where 458 and 476 cm^{-1} bands were assigned to the symmetric stretching of SSS.[53] It is noteworthy that these frequencies can potentially be shifted in peptides. Kimbaris et al.[55] have reported the GC/MS and Raman spectra of garlic oil, which contains a variety of compounds with SS and SSS groups. We noticed an intense band at 489 cm^{-1} in these spectra that could potentially originate from an SSS moiety, although the assignment of the band was not discussed in the article. Overall, our hypothetical assignment of the 490 cm^{-1} Raman band to the SSS moiety is in agreement with data from the literature.[51,53] The mechanism of SSS formation in proteins is unclear despite the significant interest that this topic has gained in recent years.[21,23,25] There is emerging evidence indicating that sulfane sulfur (S^0), which is generated from H_2S,[56] is responsible for sulfuration through the formation of persulfide or trisulfide in proteins.[56−58] It would be interesting to investigate whether these SSS form by intra- or intermolecular processes. We are currently testing this hypothesis.

It is noteworthy that the 490 cm^{-1} Raman band cannot be assigned to RSSH groups. These groups could form as a result of disulfide bond reduction in the presence of H_2S by a process known as sulfuration or sulfhydration.[59] However, R−SH and R−SSH groups have a characteristic Raman band at 2575 cm^{-1} which is not evident in the experimental spectra (Figures S1 and S2). In addition, these groups do not have a vibrational mode at 490 cm^{-1}.[35] There is evidence in the literature that indicates the possibility of SS bond reduction in the presence of H_2S and the formation of RSSH groups in basic environments. We describe the process under acidic conditions. The results allowed us to eliminate RSSH as a possible candidate for newly formed species with a characteristic 490 cm^{-1} Raman band.

Mechanism of HEWL Aggregation vs Fibrillation. Approximately 50% of all extracellular proteins have disulfide bridges.[46] SS bonds preserve the three-dimensional structure of proteins, and their cleavage typically results in significant disruption of the native conformations of proteins.[43] It is well established that SS bonds play a significant role in amyloid fibrillation.[60] Dobson and colleagues have reported that the reduction of SS bridges significantly accelerated the rate of human lysozyme aggregation.[46] It has also been demonstrated that reduction of four SS bonds to three SS bonds of apo-α-LA accelerates its fibrillation and leads to the formation of a new fibril polymorph with a different morphology and structure compared to fibrils formed from the wild-type LA.[43] At the same time, SS bonds of insulin remain intact and preserve their conformation during the fibrillation process.[60] Similar to insulin, the conformation of the SS bonds in HEWL remains intact during the fibrillation of HEWL in control solution, as we have described here.

It has been suggested that a partial denaturation of lysozyme precedes fibril formation[61] because the native tertiary structure would not allow rearrangement to the cross-β-sheet structure due to steric constraints.[8] It has also been reported that partial denaturation, the first step of lysozyme fibrillation, is an irreversible process.[32] At the same time, a fully denatured lysozyme forms amorphous aggregates that prevent fibril formation.[49] It is believed that the fully denatured protein lacks the hydrophobic side chains present in partially unordered intermediates. In addition, amorphous aggregates potentially decrease the effective concentration of HEWL available for fibril formation.[49] In agreement with these observations, our results suggest that lysozyme denatures strongly in the presence of H_2S and forms unordered aggregates that prevent β-sheet formation and fibrillation.

CONCLUSIONS

Amyloid fibrils are associated with many neurodegenerative diseases including Alzheimer's, Parkinson's, and systemic

DOI: 10.1021/jp508471v
J. Phys. Chem. B 2015, 119, 1265−1274

amyloidosis. It has recently been found that there is a reduced amount of hydrogen sulfide (H_2S) in the brain tissue of patients with Alzheimer's disease,[9] leading us to investigate the effects of H_2S on the formation of amyloid fibrils. Our objective was to utilize several complementary techniques, including Raman spectroscopy, AFM, and intrinsic tryptophan and ThT fluorescence for studying the kinetics of HEWL fibrillation, a well-characterized model amyloidogenic protein, in the presence of H_2S. Lysozyme forms typical β-sheet-rich fibrils after incubation in 20% acetic acid solution at 60 °C for approximately 70 min. The addition of 12 mM H_2S in a molar ratio of 5:1 (H_2S:HEWL) completely prevented the formation of the β-sheet conformation as measured by deep UV resonance Raman (DUVRR) spectroscopy and ThT fluorescence. By contrast, the melting of the α-helix resulted in unordered protein in the form of spherical aggregates, which were distinctly different from amyloid fibrils. According to the intrinsic tryptophan fluorescence, HEWL exhibited a more significant perturbation of its tertiary structure in the presence of H_2S than that which occurred during the partial protein denaturation at the early stage of fibrillation.

Lysozyme has four SS bonds, which stay intact during the fibrillation process. However, based on our data from nonresonance Raman spectroscopy, SS bonds exhibit significant rearrangements in the presence of H_2S. The peak area of the 507 cm^{-1} Raman band corresponding to the SS segment in the g-g-g conformation[35] was reduced significantly, and a new band appeared at 490 cm^{-1}. We assigned this new band to the SSS group based on previously reported data, the Raman spectra we acquired for model compounds, and LC-MS analysis of TCEP reduction products. Cytotoxicity tests revealed that the spherical aggregates formed by lysozyme in the presence of H_2S are nontoxic to cells by contrast with fibrils.

Overall, we report for the first time that H_2S prevents fibrillation of HEWL *in vitro* and results in the formation of small spherical aggregates of unordered protein. We also hypothesize that the mechanism of this H_2S effect involves the formation of SSS bridges. Further study is necessary to understand the detailed mechanism of this phenomenon.

Our findings that H_2S inhibits fibril formation and that putative SSS forms open a new and intriguing topic of biochemical and biomedical research. The fact that the spherical aggregates formed are nontoxic to cells by contrast with fibrils is worth further investigation *in vivo*. Given that there are new drugs under development for a slow release of H_2S with a variety of therapeutic targets, including S-sildenafil for urological conditions, S-diclofenac for inflammation, S-latanoprost for neurodegenerative illnesses, S-levodopa for Parkinson's disease, and S-aspirin for cardiovascular conditions,[62] our results suggest possible new roles of SSS *in vivo*.[23]

■ ASSOCIATED CONTENT

Ⓢ Supporting Information

Figure 1S: nonresonance Raman spectra of pure cysteine (solid line) and in the presence of H_2S at pH 7.5 (dotted line). The inset of the 2650−2350 cm^{-1} region corresponds to cysteine in the presence of H_2S (cysteine persulfide). We did not include the SH from pure cysteine because this band is too intense, and we were more interested in the SSH motif. Figure 2S: nonresonance Raman spectra of native HEWL (blue line) and HEWL incubated with H_2S at 60 °C, pH 2, for 90 min (black line). The inset corresponds to the 2350−2650 cm^{-1} region; SH vibration is not detected in native HEWL or HEWL incubated with H_2S. This material is available free of charge via the Internet at http://pubs.acs.org.

■ AUTHOR INFORMATION

Corresponding Authors

*E-mail ilednev@albany.edu (I.K.L.).
*E-mail juan.lopez16@upr.edu (J.L.-G.).

Author Contributions

⊥The first two authors contributed equally.

Author Contributions

M.F.R.-A. and T.Q.-R. contributed equally.

Notes

The authors declare no competing financial interest.

■ ACKNOWLEDGMENTS

This work was supported in part by the National Science Foundation under Award CHE-1152752 (I.K.L.), NSF PREM: Wisconsin-Puerto Rico Partnership for Research and Education in Materials (Award DMR-0934115, J.L.G) and the NIH-INBRE (Award P20GM103475-13, J.L.G.).

■ ABBREVIATIONS

H_2S, hydrogen sulfide; HEWL, hen egg white lysozyme; DUVRR, deep ultraviolet resonance Raman; AFM, atomic force microscopy; ThT, thioflavin T; cys, cysteine; SOD superoxide dismutase; hGH, human growth hormone; DPDS, dipropyl disulfide; DPTS, dipropyl trisulfide; DTT, dithiothreitol; TCEP, tris(2-carboxyethyl)phosphine.

■ REFERENCES

(1) Serpell, L. C. Alzheimer's amyloid fibrils: structure and assembly. *Biochim. Biophys. Acta, Mol. Basis Dis.* **2000**, *1502*, 16−30.
(2) Conway, K. A.; Harper, J. D.; Lansbury, P. T., Jr. Fibrils formed in vitro from alpha-synuclein and two mutant forms linked to Parkinson's disease are typical amyloid. *Biochemistry* **2000**, *39*, 2552−63.
(3) Kantcheva, R. B.; Mason, R.; Giorgini, F. Aggregation-prone proteins modulate huntingtin inclusion body formation in yeast. *PLoS Curr. Huntington's Dis.* **2014**, *6*, 1−11.
(4) Glenner, G. G. Amyloid deposits and amyloidosis. The beta-fibrilloses (first of two parts). *N. Engl. J. Med.* **1980**, *302*, 1283−92.
(5) Blake, C.; Serpell, L. Synchrotron X-ray studies suggest that the core of the transthyretin amyloid fibril is a continuous beta-sheet helix. *Structure* **1996**, *4*, 989−98.
(6) Lednev, I. K. Amyloid fibrils: the eighth wonder of the world in protein folding and aggregation. *Biophys. J.* **2014**, *106*, 1433−5.
(7) Uversky, V. N.; Li, J.; Fink, A. L. Evidence for a partially folded intermediate in alpha-synuclein fibril formation. *J. Biol. Chem.* **2001**, *276*, 10737−44.
(8) Uversky, V. N.; Fink, A. L. Conformational constraints for amyloid fibrillation: the importance of being unfolded. *Biochim. Biophys. Acta, Proteins Proteomics* **2004**, *1698*, 131−153.
(9) Eto, K.; Asada, T.; Arima, K.; Makifuchi, T.; Kimura, H. Brain hydrogen sulfide is severely decreased in Alzheimer's disease. *Biochem. Biophys. Res. Commun.* **2002**, *293*, 1485−1488.
(10) Wang, R. Physiological implications of hydrogen sulfide: a whiff exploration that blossomed. *Physiol. Rev.* **2012**, *92*, 791−896.
(11) Pietri, R.; Roman-Morales, E.; Lopez-Garriga, J. Hydrogen sulfide and hemeproteins: knowledge and mysteries. *Antioxid. Redox Signaling* **2011**, *15*, 393−404.
(12) Fukuto, J. M.; Carrington, S. J.; Tantillo, D. J.; Harrison, J. G.; Ignarro, L. J.; Freeman, B. A.; Chen, A.; Wink, D. A. Small molecule signaling agents: The integrated chemistry and biochemistry of nitrogen oxides, oxides of carbon, dioxygen, hydrogen sulfide, and their derived species. *Chem. Res. Toxicol.* **2012**, *25*, 769−793.

DOI: 10.1021/jp508471v
J. Phys. Chem. B 2015, 119, 1265−1274

(13) Blackstone, E.; Morrison, M.; Roth, M. B. H_2S induces a suspended animation-like state in mice. *Science* **2005**, *308*, 518.
(14) Li, L.; Rose, P.; Moore, P. K. Hydrogen sulfide and cell signaling. *Annu. Rev. Pharmacol. Toxicol.* **2011**, *51*, 169−87.
(15) Benavides, G. A.; Squadrito, G. L.; Mills, R. W.; Patel, H. D.; Isbell, T. S.; Patel, R. P.; Darley-Usmar, V. M.; Doeller, J. E.; Kraus, D. W. Hydrogen sulfide mediates the vasoactivity of garlic. *Proc. Natl. Acad. Sci. U. S. A.* **2007**, *104*, 17977−17982.
(16) Chauhan, N. B. Effect of aged garlic extract on APP processing and tau phosphorylation in Alzheimer's transgenic model Tg2576. *J. Ethnopharmacol.* **2006**, *108*, 385−394.
(17) Arosio, P.; Vendruscolo, M.; Dobson, C. M.; Knowles, T. P. J. Chemical kinetics for drug discovery to combat protein aggregation diseases. *Trends Pharmacol. Sci.* **2014**, *35*, 127−135.
(18) Kayed, R.; Head, E.; Sarsoza, F.; Saing, T.; Cotman, C. W.; Necula, M.; Margol, L.; Wu, J.; Breydo, L.; Thompson, J. L.; et al. Fibril specific, conformation dependent antibodies recognize a generic epitope common to amyloid fibrils and fibrillar oligomers that is absent in prefibrillar oligomers. *Mol. Neurodegener.* **2007**, *2*, 18.
(19) Kurouski, D.; Luo, H.; Sereda, V.; Robb, F. T.; Lednev, I. K. Rapid degradation kinetics of amyloid fibrils under mild conditions by an archaeal chaperonin. *Biochem. Biophys. Res. Commun.* **2012**, *422*, 97−102.
(20) Ravi, V. K.; Goel, M.; Kotamarthi, H. C.; Ainavarapu, S. R. K.; Swaminathan, R. Preventing disulfide bond formation weakens non-covalent forces among lysozyme aggregates. *PLoS One* **2014**, *9*, e87012.
(21) Gu, S.; Wen, D.; Weinreb, P. H.; Sun, Y.; Zhang, L.; Foley, S. F.; Kshirsagar, R.; Evans, D.; Mi, S.; Meier, W.; et al. Characterization of trisulfide modification in antibodies. *Anal. Biochem.* **2010**, *400*, 89−98.
(22) Ogasawara, Y.; Isoda, S.; Tanabe, S. Tissue and subcellular distribution of bound and acid-labile sulfur, and the enzymic capacity for sulfide production in the rat. *Biol. Pharm. Bull.* **1994**, *17*, 1535−42.
(23) Nielsen, R. W.; Tachibana, C.; Hansen, N. E.; Winther, J. R. Trisulfides in proteins. *Antioxid. Redox Signaling* **2011**, *15*, 67−75.
(24) David, C.; Foley, S.; Enescu, M. Protein S-S bridge reduction: a Raman and computational study of lysozyme interaction with TCEP. *Phys. Chem. Chem. Phys.* **2009**, *11*, 2532−42.
(25) Cumnock, K.; Tully, T.; Cornell, C.; Hutchinson, M.; Gorrell, J.; Skidmore, K.; Chen, Y.; Jacobson, F. Trisulfide modification impacts the reduction step in antibody−drug conjugation process. *Bioconjugate Chem.* **2013**, *24*, 1154−1160.
(26) Xu, M.; Ermolenkov, V. V.; Uversky, V. N.; Lednev, I. K. Hen egg white lysozyme fibrillation: a deep-UV resonance Raman spectroscopic study. *J. Biophotonics* **2008**, *1*, 215−229.
(27) Mosmann, T. Rapid colorimetric assay for cellular growth and survival: Application to proliferation and cytotoxicity assays. *J. Immunol. Methods* **1983**, *65*, 55−63.
(28) Copeland, R. A.; Spiro, T. G. Ultraviolet resonance Raman spectra of cytochrome c conformational states. *Biochemistry* **1985**, *24*, 4960−4968.
(29) Myshakina, N. S.; Asher, S. A. Peptide bond vibrational coupling. *J. Phys. Chem. B* **2007**, *111*, 4271−4279.
(30) Wang, Y.; Purrello, R.; Jordan, T.; Spiro, T. G. UVRR spectroscopy of the peptide bond. 1. Amide S, a nonhelical structure marker, is a C.alpha.H bending mode. *J. Am. Chem. Soc.* **1991**, *113*, 6359−6368.
(31) Xu, M.; Ermolenkov, V. V.; He, W.; Uversky, V. N.; Fredriksen, L.; Lednev, I. K. Lysozyme fibrillation: Deep UV Raman spectroscopic characterization of protein structural transformation. *Biopolymers* **2005**, *79*, 58−61.
(32) Xu, M.; Shashilov, V.; Lednev, I. K. Probing the cross-β core structure of amyloid fibrils by hydrogen−deuterium exchange deep ultraviolet resonance Raman spectroscopy. *J. Am. Chem. Soc.* **2007**, *129*, 11002−11003.
(33) Lednev, I. K., Vibrational spectroscopy: Biological applications of ultraviolet Raman spectroscopy. In *Protein Structures, Methods in Protein Structures and Stability Analysis*; Uversky, V. N., Permyakov, E. A., Eds.; Nova Science Publishers, Inc.: New York, 2007.
(34) Asher, S. A.; Ianoul, A.; Mix, G.; Boyden, M. N.; Karnoup, A.; Diem, M.; Schweitzer-Stenner, R. Dihedral ψ angle dependence of the amide III vibration: A uniquely sensitive UV resonance Raman secondary structural probe. *J. Am. Chem. Soc.* **2001**, *123*, 11775−11781.
(35) Tu, A. T. *Raman Spectroscopy in Biology: Principles and Applications*; Wiley: New York, 1982.
(36) Lednev, I.; Ermolenkov, V.; He, W.; Xu, M. Deep-UV Raman spectrometer tunable between 193 and 205 nm for structural characterization of proteins. *Anal. Bioanal. Chem.* **2005**, *381*, 431−437.
(37) Oladepo, S. A.; Xiong, K.; Hong, Z.; Asher, S. A.; Handen, J.; Lednev, I. K. UV resonance Raman investigations of peptide and protein structure and dynamics. *Chem. Rev.* **2012**, *112*, 2604−2628.
(38) Imoto, T.; Forster, L. S.; Rupley, J. A.; Tanaka, F. Fluorescence of lysozyme: Emissions from tryptophan residues 62 and 108 and energy migration. *Proc. Natl. Acad. Sci. U. S. A.* **1972**, *69*, 1151−1155.
(39) Pajot, P. Fluorescence of proteins in 6-M guanidine hydrochloride. *FEBS J.* **1976**, *63*, 263−269.
(40) Van Wart, H. E.; Lewis, A.; Scheraga, H. A.; Saeva, F. D. Disulfide bond dihedral angles from Raman spectroscopy. *Proc. Natl. Acad. Sci. U. S. A.* **1973**, *70*, 2619−23.
(41) Nakanishi, M.; Takesada, H.; Tsuboi, M. Conformation of the cystine linkages in bovine α-lactalbumin as revealed by its Raman effect. *J. Mol. Biol.* **1974**, *89*, 241−243.
(42) Kocherbitov, V.; Latynis, J.; Misiūnas, A.; Barauskas, J.; Niaura, G. Hydration of lysozyme studied by Raman spectroscopy. *J. Am. Chem. Soc.* **2013**, *117*, 4981−4992.
(43) Kurouski, D.; Lednev, I. K. The impact of protein disulfide bonds on the amyloid fibril morphology. *Int. J. Nanosci. Nanotechnol.* **2011**, *2*, 167−176.
(44) Burns, J. A.; Butler, J. C.; Moran, J.; Whitesides, G. M. Selective reduction of disulfides by tris(2-carboxyethyl)phosphine. *J. Org. Chem.* **1991**, *56*, 2648−2650.
(45) Harpp, D. N.; Smith, R. A. Sulfur-sulfur bond cleavage processes. Selective desulfurization of trisulfides. *J. Am. Chem. Soc.* **1982**, *104*, 6045−6053.
(46) Mossuto, M. F.; Bolognesi, B.; Guixer, B.; Dhulesia, A.; Agostini, F.; Kumita, J. R.; Tartaglia, G. G.; Dumoulin, M.; Dobson, C. M.; Salvatella, X. Disulfide bonds reduce the toxicity of the amyloid fibrils formed by an extracellular protein. *Angew. Chem., Int. Ed.* **2011**, *50*, 7048−51.
(47) Dobson, C. M. Protein folding and misfolding. *Nature* **2003**, *426*, 884−890.
(48) Powers, E. T.; Powers, D. L. Mechanisms of protein fibril formation: Nucleated polymerization with competing off-pathway aggregation. *Biophys. J.* **2008**, *94*, 379−391.
(49) Wang, S. S.; Liu, K.-N.; Wang, B.-W. Effects of dithiothreitol on the amyloid fibrillogenesis of hen egg-white lysozyme. *FBES J.* **2010**, *39*, 1229−1242.
(50) Sugeta, H.; Go, A.; Miyazawa, T. Vibrational spectra and molecular conformations of dialkyl disulfides. *Bull. Chem. Soc. Jpn.* **1973**, *46*, 3407−11.
(51) Freeman, S. K. Applications of laser Raman spectroscopy to natural products research. *J. Agric. Food Chem.* **1973**, *21*, 521−525.
(52) Rebouças, J. S.; Patrick, B. O.; James, B. R. Thiol, disulfide, and trisulfide complexes of Ru porphyrins: potential models for iron-sulfur bonds in heme proteins. *J. Am. Chem. Soc.* **2012**, *134*, 3555−70.
(53) Janz, G. J.; Roduner, E.; Coutts, J. W.; Downey, J. R. Raman studies of sulfur-containing anions in inorganic polysulfides. Barium trisulfide. *Inorg. Chem.* **1976**, *15*, 1751−1754.
(54) Wieser, H.; Krueger, P. J.; Muller, E.; Hyne, J. B. Vibrational spectra and a force field for H_2S_3 and H_2S_4. *Can. J. Chem.* **1969**, *47*, 1633−1637.
(55) Kimbaris, A. C.; Siatis, N. G.; Pappas, C. S.; Tarantilis, P. A.; Daferera, D. J.; Polissiou, M. G. Quantitative analysis of garlic (Allium sativum) oil unsaturated acyclic components using FT-Raman spectroscopy. *Food Chem.* **2006**, *94*, 287−295.
(56) Toohey, J. I. Sulfur signaling: is the agent sulfide or sulfane? *Anal. Biochem.* **2011**, *413*, 1−7.

DOI: 10.1021/jp508471v
J. Phys. Chem. B 2015, 119, 1265−1274

(57) Greiner, R.; Palinkas, Z.; Basell, K.; Becher, D.; Antelmann, H.; Nagy, P.; Dick, T. P. Polysulfides link H_2S to protein thiol oxidation. *Antioxid. Redox Signaling* **2013**, *19*, 1749−65.
(58) Kimura, H. The physiological role of hydrogen sulfide and beyond. *Nitric Oxide* **2014**, *41*, 4−10.
(59) Kabil, O.; Banerjee, R. Redox biochemistry of hydrogen sulfide. *J. Biol. Chem.* **2010**, *285*, 21903−7.
(60) Kurouski, D.; Washington, J.; Ozbil, M.; Prabhakar, R.; Shekhtman, A.; Lednev, I. K. Disulfide bridges remain intact while native insulin converts into amyloid fibrils. *PLoS One* **2012**, *7*, e36989.
(61) Booth, D. R.; Sunde, M.; Bellotti, V.; Robinson, C. V.; Hutchinson, W. L.; Fraser, P. E.; Hawkins, P. N.; Dobson, C. M.; Radford, S. E.; Blake, C. C. F.; et al. Instability, unfolding and aggregation of human lysozyme variants underlying amyloid fibrillogenesis. *Nature* **1997**, *385*, 787−793.
(62) Sparatore, A.; Santus, G.; Giustarini, D.; Rossi, R.; Del Soldato, P. Therapeutic potential of new hydrogen sulfide-releasing hybrids. *Expert Rev. Clin. Pharmacol.* **2010**, *4*, 109−121.

DOI: 10.1021/jp508471v
J. Phys. Chem. B 2015, 119, 1265−1274